

DEVELOPMENT AND EXPERIMENTAL VALIDATION OF A
LOW-COST PHOTOLITHOGRAPHY STEPPER

by

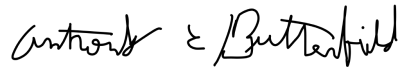
John Peterson

A Senior Honors Thesis Submitted to the Faculty of
The University of Utah
In Partial Fulfillment of the Requirements for the
Honors Degree in Bachelor of Science

In

Chemical Engineering

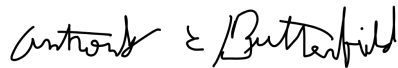
Approved:



Anthony Butterfield, Ph.D.
Thesis Faculty Supervisor



Eric Eddings, Ph.D.
Chair, Department of Chemical
Engineering



Anthony Butterfield, Ph.D.
Honors Faculty Advisor

Monisha Pasupathi, Ph.D.
Dean, Honors College

March 2025
Copyright © 2025
All Rights Reserved

ABSTRACT

Photolithography is an essential process in the semiconductor industry. It is the method by which the transistor has chased Moore's law from the centimeter realm to the nanometer realm, a multi-millionfold reduction over the last 60 years. This continuous scaling has underpinned the rapid evolution of modern technology as access to ever increasing computational power has become a widespread commodity. Traditional tools for this process prove to be cost-prohibitive and bar those without large financial backing from exploring the potential applications of photolithography. We propose and construct a low-cost desktop-scale maskless photolithography stepper based on designs by the open source group HackerFab and validate its functionality by patterning UV curable resin. A digital micromirror device (DMD) is used to produce patterns without need for development of physical masks, increasing the variability and versatility of the device. We demonstrate the system's capability by producing features on the order of 10 μm and discuss its potential as an accessible educational and research tool for environments without conventional nanofabrication facilities.

TABLE OF CONTENTS

ABSTRACT	ii
1 INTRODUCTION	1
2 METHODS	7
2.1 OPTICS	7
2.1.1 LIGHT SOURCE	9
2.1.2 PATTERNING	11
2.1.3 FOCUSING	12
2.2 XYZ STAGE	13
2.3 SPINCOATER	14
2.4 SOFTWARE	16
3 RESULTS	18
4 DISCUSSION	22
BIBLIOGRAPHY	31

1 - INTRODUCTION

In the mid 1820s, Nicéphore Niépce first used Bitumen of Judea—a naturally occurring, light-sensitive asphalt that becomes less soluble upon exposure to light—to capture the world’s first permanent photograph [1]. Though the term ”photoresist” itself wasn’t used until much later, Bitumen of Judea effectively functioned as the earliest known material with photoresistive properties. A major advancement occurred over a century later, in 1940, when Oskar Süß created diazonaphthoquinone, marking the development of the first synthetic positive photoresist [2]. Its positive classification denoting that, unlike a negative photoresist such as Bitumen of Judea, diazonaphthoquinone’s solubility increases upon exposure to light.

Building on this technology, Jay W. Lathrop and James R. Nall at the National Bureau of Standards developed techniques for miniaturizing circuitry by using photoresist to pattern and etch germanium semiconductor devices in 1957–1958 [3]. They produced the first photolithographic transistors and introduced the term ”photolithography,” a term used interchangeably with lithography in the context of semiconductor fabrication. Concurrently, in 1957, Jules Andrus at Bell Laboratories secured a foundational patent for photolithographic processes in semiconductor manufacturing [4]. This patent set the stage for photolithography to become one of today’s most precise, complex, and critical manufacturing techniques worldwide.

At its core, photolithography introduces a fundamentally different approach to manufacturing surfaces. Traditional techniques such as drilling, milling, or sanding are constrained by mechanical limits such as tool sharpness, heat dissipation, and the physical

properties of the material. In contrast, photolithography uses light to define patterns in photosensitive chemicals, shifting the resolution limits from mechanical restrictions to optical and chemical ones. The ultimate boundaries are no longer defined by how fine a cutting edge is ground, but by how finely light can be controlled and how sensitively the photoresist responds.

The modern photolithography process, while far more advanced, still echoes the principles explored by Niépce and other early chemists. It is part of a larger sequence of steps, but the photolithography stage itself can be broken down into a few key operations. First, a thin film of photoresist is applied to the wafer surface, typically using a method called spin coating, which ensures uniform thickness across the substrate [5]. Next, the coated wafer is placed into a stepper or scanner machine that projects a precisely defined light pattern onto the resist through a photomask. Depending on whether a positive or negative resist is used, the exposed (or unexposed) regions become soluble in a developer solution and are washed away.

This leaves behind a patterned resist layer that acts as a physical barrier, protecting specific areas of the underlying material. Subsequent processing steps like etching, ion implantation, or thin-film deposition can then selectively modify these exposed regions. Once these steps are complete, the remaining resist is stripped away, and the wafer is ready for the next layer. Through repeated iterations, this process enables the construction of intricate, multi-layered devices with nanoscale precision.

As the global demand for smaller, faster, and more power-efficient devices has grown, the photolithography process has faced increasing pressure to print ever-finer features. This push toward miniaturization has exposed the physical limits of how small patterns can be

made using light, a challenge rooted in the wave nature of light itself. Fundamentally, the resolution of a photolithographic optic system is constrained by diffraction, often described through a simplified model known as Rayleigh's criterion [6]:

$$CD = k_1 \frac{\lambda}{NA}$$

In this expression, CD (critical dimension) represents the smallest feature that can be reliably printed, λ is the wavelength of the light source, NA is the numerical aperture of the lens system, and k_1 is a process-related constant. Improving resolution depends on reducing the wavelength, increasing the numerical aperture, or minimizing k_1 through advanced process techniques.

Over time, the industry has steadily shortened exposure wavelengths. Early systems used the 436 nm g-line of mercury lamps, followed by 365 nm i-line, then 248 nm and 193 nm deep ultraviolet (DUV) lasers. Today's most advanced processes use extreme ultraviolet (EUV) light at 13.5 nm. In parallel, lens systems with increasingly high numerical apertures have been developed. One major innovation, immersion lithography, introduced a thin layer of water between the lens and wafer to boost the numerical aperture beyond 1.0 [7].

However, improvements in optics alone are not enough. The materials used in photolithography must also be optimized to respond precisely and reliably to each new wavelength. Modern photoresists are highly engineered materials, often chemically amplified to increase sensitivity at low photon doses [8]. These resists generate acid upon exposure, which then diffuses during a post-exposure bake to catalyze solubility changes. Although this enables faster processing, it also introduces new challenges such as line edge rough-

ness, stochastic variation, and resolution loss due to acid diffusion [9].

As a result, the continued shrinking of features has become a careful balance between optical precision and chemical control. As the industry pushes resolution smaller and finer, further innovation must come not only from better optics and shorter wavelengths, but also from breakthroughs in resist chemistry, novel materials, and even entirely different patterning approaches like directed self-assembly or multi-patterning techniques [10].

Photolithography is just one step in a much larger sequence of processes that collectively define modern semiconductor manufacturing. A single chip may require dozens of lithographic exposures, each aligned with nanometer-scale precision to the previous layers. Between these exposures, other steps such as deposition, etching, doping, and cleaning are used to physically build and modify the device structure.

Although these supporting processes are critical, it is photolithography that sets the spatial blueprint for each layer, defining where material should be added, removed, or altered in the surrounding processes. The quality of each lithographic pattern not only determines the final dimensions of a feature but also influences the yield, performance, and scalability of the device. As feature sizes shrink and layer counts grow, photolithography increasingly dictates the feasibility and economics of the entire manufacturing process.

Despite its precision and power, photolithography also represents one of the most expensive and technically demanding parts of chip fabrication, with cutting-edge tools costing hundreds of millions of dollars. The high cost and complexity of photolithography create significant barriers to entry, especially for educational institutions, research groups, or startups without access to industrial-scale infrastructure. For example, a state-of-the-art High-NA EUV lithography system from ASML is predicted to cost roughly \$350 million

[11], requiring not only substantial capital but also highly specialized maintenance and support. Beyond the exposure tool itself, lithography demands cleanroom environments with rigorous particulate control to avoid pattern defects. These facilities can cost tens of millions of dollars to construct and operate, adding to the overhead of any lithography-based fabrication.

Another challenge lies in the trade-offs between throughput and resolution. High-resolution lithography methods often involve slower exposure times or more complex patterning strategies (e.g., multiple patterning), which increase cost per wafer. Conversely, faster, lower-resolution systems may not be viable for advanced node devices.

These trade-offs have given rise to distinct categories of photolithography tools, particularly in how patterns are delivered to the wafer. Broadly, systems can be classified into masked and maskless photolithography processes [12]. While most industrial workflows rely on masked systems as described above—where a physical photomask defines the projected pattern—maskless methods eliminate the mask entirely and write patterns directly onto the resist using programmable light sources such as lasers, electron beams, or digital micromirrors.

Masked photolithography is ideal for high-throughput manufacturing due to its ability to expose entire fields in parallel. However, mask fabrication is both expensive and time-intensive, with advanced mask sets costing millions of dollars [13]. This makes masked approaches less flexible for rapid prototyping or small-scale production.

Maskless photolithography, on the other hand, offers greater design flexibility and lower upfront costs by avoiding the need for masks altogether. Techniques such as electron beam lithography provide exceptional resolution for research applications but are limited by their

slower writing speeds. Digital light processing (DLP) lithography offers a middle ground, using block exposure with dynamically programmable patterns to enable flexible, moderately high-resolution exposures, making it well-suited for educational and desktop-scale systems [14].

These numerous financial and technical constraints have made photolithography a persistent bottleneck in accessible microfabrication. While critical to device fabrication, the high capital costs, infrastructural requirements, and reliance on complex mask sets place this technology out of reach for many academic institutions, small research groups, and early-stage innovators. This has created a growing disparity between those with access to advanced lithographic capabilities and those without, limiting the pace and diversity of innovation in fields reliant on microscale patterning.

In response to these challenges, there is a clear and growing need for alternative lithographic approaches that reduce the economic and technical thresholds of entry. Maskless photolithography, particularly techniques utilizing digital light processing, present a compelling pathway forward. By removing the dependency on photomasks and enabling re-programmable, high-resolution exposures with lower-cost equipment, such systems offer a promising foundation for more agile and accessible patterning platforms.

The broader implication is that the advancement of lithographic methods must not only aim at pushing the frontiers of resolution and throughput, but also at expanding the accessibility of the process itself. As the demand for distributed, rapid, and small-scale fabrication increases, the development of compact, flexible, and cost-effective photolithography tools becomes an essential step toward democratizing access to microfabrication and enabling broader participation in the design and development of next-generation technologies.

2 - METHODS

The device that is described here follows work by the [HackerFab \[15\]](#) group out of Carnegie Mellon University. In particular, this corresponds to the "Lithostepper V2" design, and any and all design files mentioned as well as thorough build instructions are found on their [gitbook](#).

The device can be separated into a few categories of discussion. The optics system stands alone as does the XYZ stage with a brief discussion of its firmware. Further discussion of the optics system will be broken into subsections according to the purpose those parts of the hardware accomplish. Additionally, we constructed a DIY Spincoater for this device which will be discussed in brief. Finally we will cover the software that is used to run the device.

2.1 - OPTICS



Figure 2.1: Texas Instruments DLP471TP Evaluation Module [16]

At the heart of our lithostepper is a modified projector. The projector we use is the DLPDLCR471TPEVM shown in [Figure 2.1](#) from Texas Instruments. This projector has been chosen because, as an evaluation module, it has a GUI that allows for modification of the device firmware as well as a chassis which is easy to modify. Further motivation for the projector as a basis will be explored in the discussion of patterning.

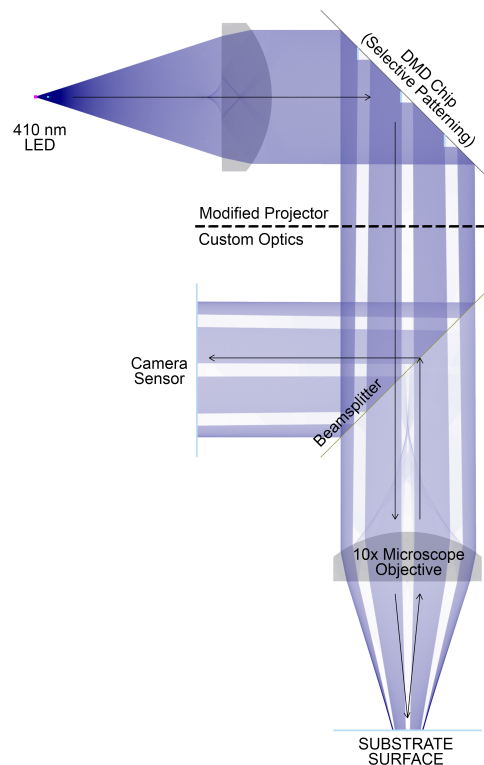


Figure 2.2: The Lithostepper V2 light path simulated in Phydemo [17]

An overview of the optical path which our device controls is given in [Figure 2.2](#). A line separating the parts that are contained in the modified projector and parts that are custom optics is included for reference in the forthcoming sections. Note that this figure is not technically accurate due to limitations of the simulation used to produce it, but serves as a visual aid in identifying the path the light takes inside of the system.

2.1.1.1 - LIGHT SOURCE

At the heart of any lithography system lies its light source, which defines the resolution limits of patterning. As described by Rayleigh's criterion, the smallest resolvable feature is proportional to the wavelength of the illuminating light: shorter wavelengths enable finer features. While the semiconductor industry is steadily advancing toward extreme ultraviolet (EUV) lithography at a wavelength of 13.5 nm, this shift comes with increasing complexity. Below approximately 365 nm, conventional glass optics begin to absorb light significantly, necessitating the use of quartz optics [18]. At even shorter wavelengths, such as EUV, nearly all materials are absorptive, requiring fully reflective optical systems based on multilayer mirrors.

In contrast, the device presented here is designed for patterning features on the micrometer scale. For this purpose, a near-ultraviolet light source at 410 nm is sufficient, enabling the use of straightforward and cost-effective transmissive optics. This choice improves system cost and accessibility without compromising the resolution goals for our intended applications. Based on the optical system design, we estimate the resolution using Rayleigh's criterion:

$$\begin{aligned}
 CD &= k_1 \frac{\lambda}{NA} \\
 &= 0.61 \frac{410nm}{0.25} \\
 &= 1000.4nm \approx 1\mu m.
 \end{aligned}$$

This calculated critical dimension represents an idealized resolution limit. In practice,

real-world factors such as optical aberrations, mechanical alignment, and resist performance may further constrain resolution. Nevertheless, it provides a valuable benchmark that informed the decision to target a practical feature size of 10 μm .

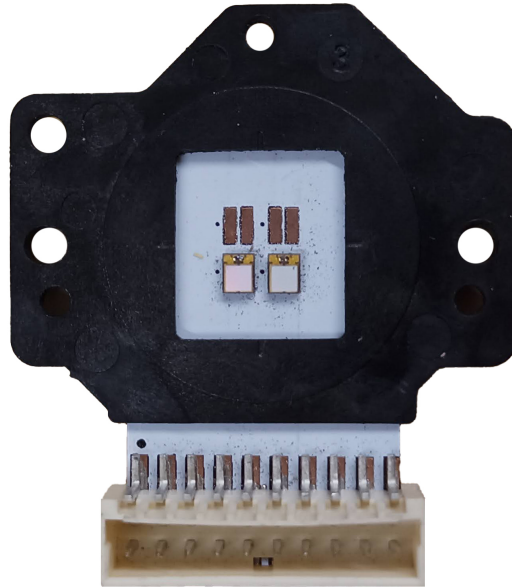


Figure 2.3: Custom copper-core PCB with 2 near-UV 410 nm LEDs

Having selected a suitable wavelength, the next step is to implement the light source. The system is built around the DLPDLCR471TPEVM projector from Texas Instruments, which employs digital light processing (DLP) as detailed in the patterning section. To match our desired wavelength, we replaced the projector's original blue LED board with a custom copper-core PCB, shown in [Figure 2.3](#), featuring two 410 nm LEDs commonly available from various suppliers. The copper-core board is essential as it conducts heat away from the LEDs to the preexisting heat sink originally used for the blue LED in order to avoid the LEDs burning out. Thus, the device has been retrofit so any signals sent over the HDMI connection on the blue channel to the projector will now be patterned in UV.

2.1.2 - PATTERNING

The selection of the projector is based on the discussion of masked versus maskless photolithography. As motivated in the introduction, generating masks can become expensive quickly, particularly if the device targets an application with a focus on variety of patterns over quantities of exposures. For such an environment, generating a physical mask every time a new pattern is needed quickly becomes expensive and cumbersome. As we would like to target those experimental environments, our device has been selected to be maskless.

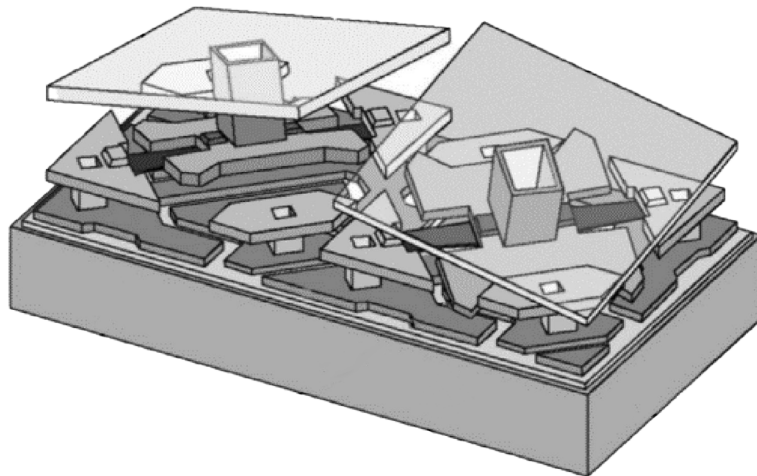


Figure 2.4: A close up view of two micromirrors on a DMD chip [19]

The Digital Light Processing (DLP) technology behind the Texas Instruments projectors features a key chip. This chip is known as a digital micromirror device (DMD) and is the reason that a projector has been chosen as the basis for this project. As can be seen in [Figure 2.4](#), the DMD chip features an array of micromirrors. Each of these mirrors can

be tilted back and forth corresponding to whether their pixel is on or off. This selectively reflects light into the optics essentially providing a digital mask of the light.

This system of micromirrors allows us to mask our light on the fly instead of needing to use a traditional stationary mask to pattern it. Thus, we are able to dynamically generate masked UV light by sending a controlled image to the projector over a standard HDMI connection. This is the power of DLP/DMD based lithography. This flexibility for quick iteration clearly motivates why a maskless approach was chosen for this application.

2.1.3 - FOCUSING

Once the light has been patterned, it exits the projector. At this point two tasks remain. First, the light must then be de-magnified. This is done using a 10x microscope objective as depicted in [Figure 2.2](#). Secondly, the light must be accurately brought into focus, a much more difficult task.

To do so, a custom optics arrangement is created to allow the focus of the surface to be determined. By putting a dichroic mirror, or beamsplitter, in front of the microscope objective, it can be oriented such that on the initial pass the beam transmits through the splitter, but upon return is redirected into a camera. This camera has been placed to match the back focal length of the microscope objective (160mm) in order to ensure the focal plane of the camera sensor is aligned with the focal plane of the surface. By viewing the reflection of the light from the surface in our camera, we are able to determine when our light is focused onto the surface.

As these connections must be precisely configured to ensure the focal planes align, the parts used are all connectors and links purchased from an optics supplier, in our case Thorlabs. This ensures precision in connection and consistency in alignment. A complete

bill of materials as well as further instructions on the parts used and assembly of this system can be found on HackerFab's instructions. The camera used in our device is the Teldyne BFS-U3-200S7C-C 20MP C-Mount camera, although the Spinnaker SDK [20] for this camera is proprietary and as such the other HackerFab collaborators are moving away from this camera towards an alternative open-source friendly solution.

2.2 - XYZ STAGE

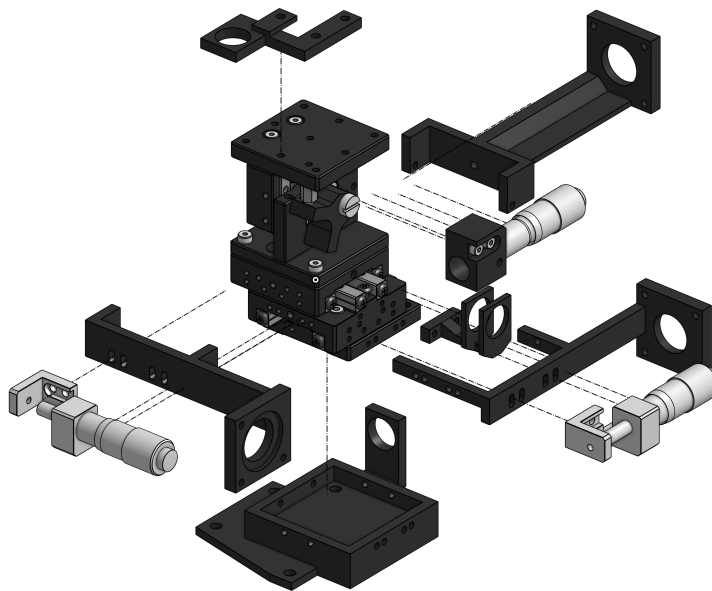


Figure 2.5: An expanded view of the parts of the XYZ stage

In recent years, trends in manufacturing have led to a surprising drop in the cost of linear precision stages. The one used in this device was purchased for approximately \$125, with even cheaper alternatives available from various suppliers. A model of the stage used is shown at the center of [Figure 2.5](#). The mechanism operates with two sets of linear rails, each connected to a spring that pulls it in one direction along its axis of movement. A micrometer, visible in silver in the figure, pushes against an L-stop by rotating along a

finely pitched thread. This setup enables precise movement of the stage against the spring tension, with two full rotations corresponding to 1 mm of displacement.

Since the purchased stage was non-motorized, significant effort went into designing 3D-printed mounts to motorize it. With motors added, it was found advantageous to implement absolute positioning. To achieve this, the mounts were modified to include capacitive proximity sensors, enabling the stage to detect a defined "home" position.

The motors are controlled using an Arduino Uno paired with a CNC shield running the open-source GRBL firmware [21]. In its basic configuration, GRBL listens to the serial port for G-Code instructions and executes them according to its firmware settings. Our setup includes a homing sequence that uses the proximity sensors as limit switches, and the virtual units are calibrated to match real-world movement. Additional implementation details, circuitry, and model files are available on the HackerFab site.

2.3 - SPINCOATER

A spincoater is a tool used to apply uniform thin films onto flat substrates by spinning them at high speeds with a liquid like photoresist—resin in our case—is dispensed onto the surface. Centrifugal force spreads the liquid evenly, and the resulting film thickness can be precisely controlled by adjusting parameters like spin speed and duration. In this project, the spincoater is a critical component, as it ensures a consistent and reproducible film layer prior to exposure. Uniform film thickness is essential for achieving high-resolution features and reliable pattern transfer during the photolithography process.



Figure 2.6: Spincoater with a gravity chuck for 22mm glass slides

The final spincoater design is incredibly simple. An old hard drive motor has been modified by attaching an 30A electronic speed controller (ESC) to each of the pads on the back. This ESC is regulated using an Arduino Nano which has custom firmware written to interface with the keypad, screen, potentiometer, and capacitive touch sensor. All of this is mounted inside a 3D printed case designed to fit the hard drive. The firmware is incredibly simple and features two menus, one for the setting of speed, and one for the tuning of PID parameters. The PID parameters for our speed control are determined to just slightly overshoot the setpoint being a relatively rapid response. The range of operation for our device is 2,000-10,000 RPM at a total cost of \$35.

2.4 - SOFTWARE

In order to operate the device a custom software solution has been developed. The software is created using a Python backend with the Tkinter module as the graphics framework. The software interfaces with the XYZ stage over the serial monitor sending G-Code over the connection to the Arduino. Additionally, it interacts with the Teldyne camera over their proprietary Spinnaker API. Further implementation details can be found with the [source code](#) [22] which remains in active development.

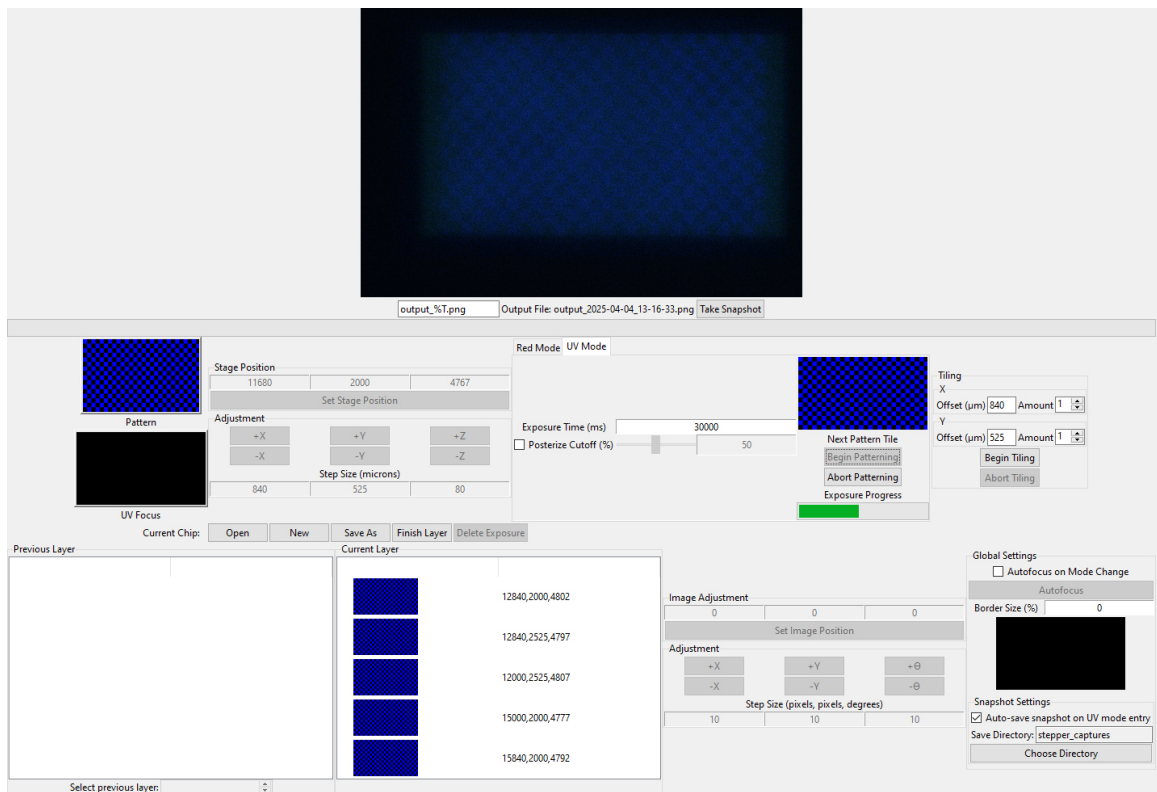


Figure 2.7: Screenshot of the custom tkinter based software in UV mode

A screenshot of the software in use is provided in [Figure 2.7](#). Most notably, is the live camera preview in the top center of the screen. This allows for the device to be focused—as discussed in the section 2.1.3—to be focused both manually and automatically by using a

Sobel edge detection algorithm to score the focus of the image [23]. Additionally, a pattern for exposure can be loaded into the "Pattern" section on the middle left as well as a pattern used to focus the UV light in the "UV Focus" box.

Continuing right from there, the XYZ stage can then be controlled using the "Stage Position" portion of the controls. Next, the "Red Mode" and "UV Focus" mode allow for the device to be focused and swapped into "UV Mode" which turns on the custom UV LEDs to pattern our device. A set time is selected before "Begin Patterning" sends the full pattern to be exposed to the projector for that amount of time. An experimental tiling section is also featured with the goal of tessellating patterns across a surface.

Moving down to the bottom left now, the "Previous/Current Layer" sections can be found. As the device was designed with the intent of multilayer lithography, this system is in place to allow for a user to etch a surface, finish a layer, and then add a second (or any numbered) layer of photoresist and repeat an etch. This system tracks the location of each of the etches in order to allow the user to return to those positions for future overlays and saves the "chip file" to a .json file. Finally, the bottom right features functionality designed for digitally adjusting the pattern to align with overlay in case the chip is seated slightly different between etch layers.

3 - RESULTS

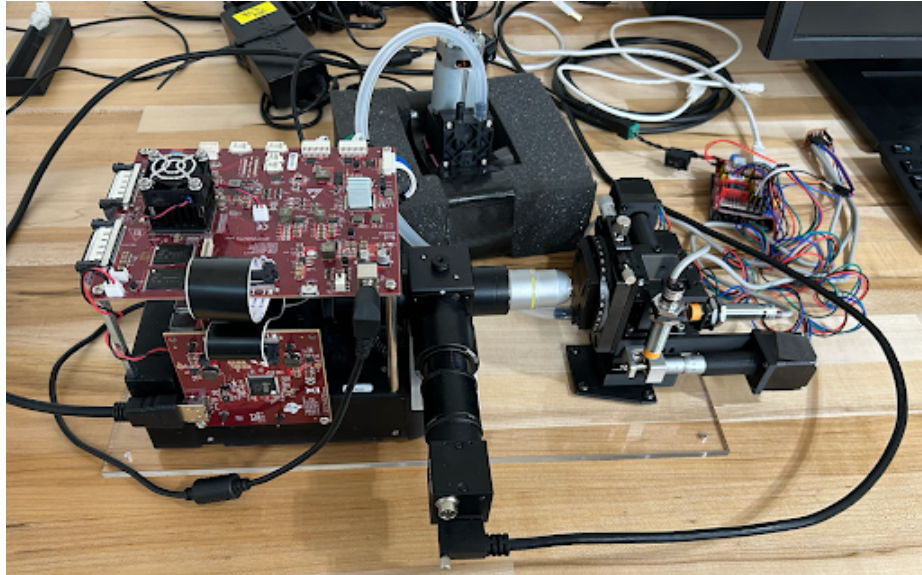


Figure 3.1: The completed Lithostepper V2

The work has resulted in the completed stepper shown in [Figure 3.1](#). Comparing it to [Figure 2.2](#), the individual parts can be determined from left to right: modified projector, custom beamsplitter / magnifier optics, and XYZ stage. Because of the lab we this work was accomplished in, photoresist would have been a hassle to work with so our group decided to proof the device using a less toxic chemical and turned to UV curable 3D printer resin cured onto glass slides, specifically Anycubic Standard Black Resin V2. This selection was made based on the sensitivity of the resin to the wavelength produced by our device, as well as the ability to work with it outside of a fume hood. Note however, that this selection of resin instead of a traditional photoresist significantly limited our ability to resolve fine details and patterns.

Our procedure resulted from much trial and error and is thus included in discussion of

results rather than methods, noting that room remains for improvement. The procedure with this resin involved a 2000 RPM spin coat to get a roughly 50 μm film thickness, followed by a 30 second etch time for each pattern. Finally, once exposed, the uncured resin was washed away using isopropanol leaving behind the pattern we exposed. In essence the resin in this process acts as a negative photoresist.

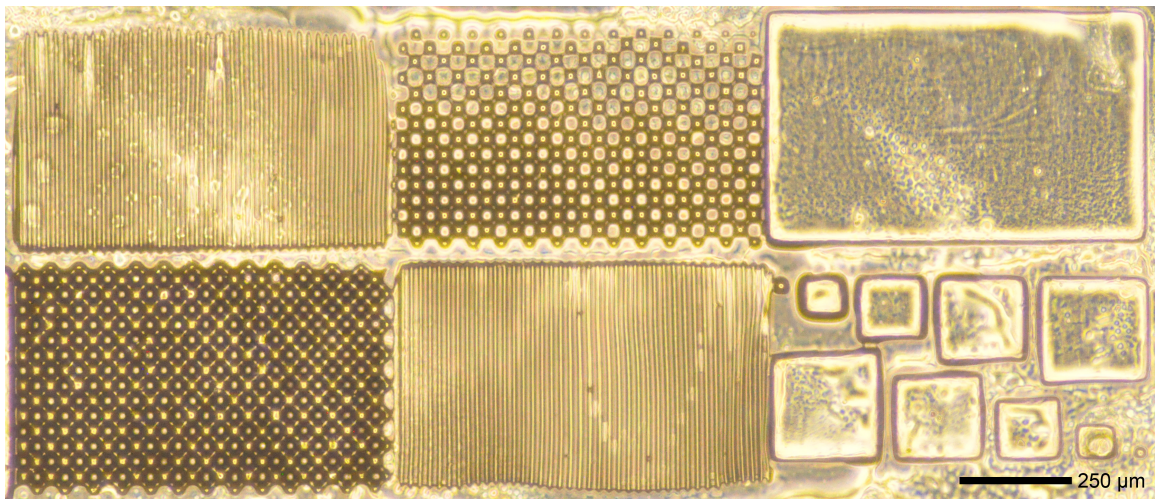


Figure 3.2: A multi pattern etch showing off the pattern changing and tiling functions

Patterns from a successful etch can be viewed under visual microscopy or scanning electron microscopy (SEM.) An example etch of multiple patterns tiled across the surface can be seen in [Figure 3.2](#). By using the known distance between etches, as the XYZ stage positioning is accurate to a few microns, the ImageJ [\[24\]](#) software can use this scale and digitally convert from pixels to μm s. This yields an exposure size of roughly 840 x 525 μm s.

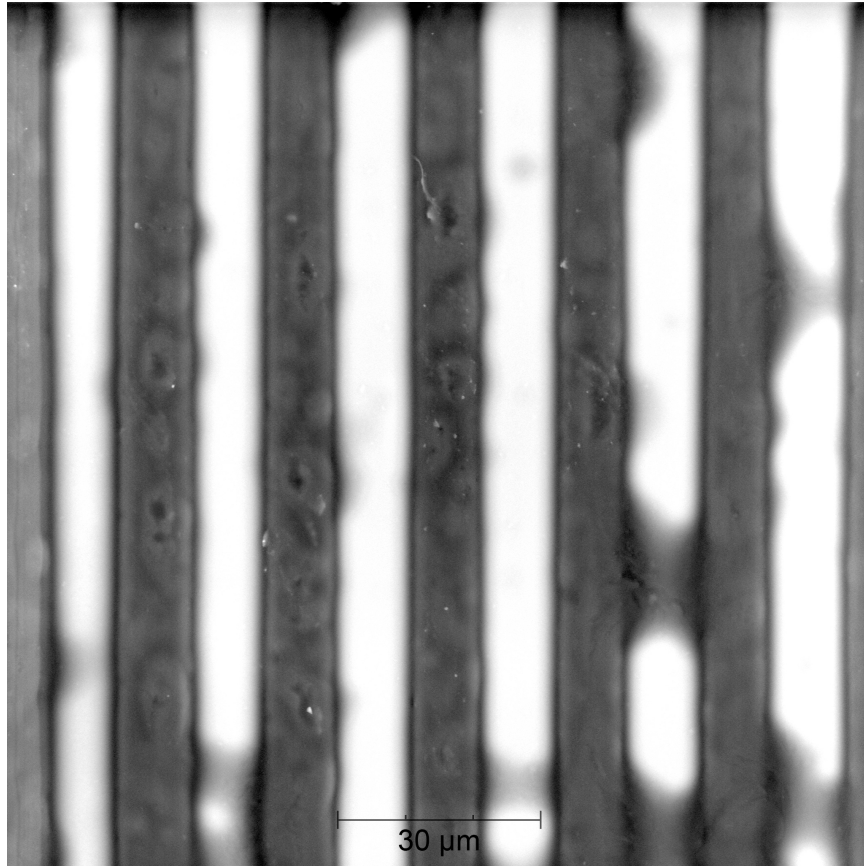


Figure 3.3: 10 μm fine line exposure under BSD SEM

A close up view of the fine line exposure from [Figure 3.2](#) can be viewed in SEM to determine a better understanding of etch quality. Shown in [Figure 3.3](#) is the backscattering detection (BSD) mode of the SEM with a scale bar demonstrating somewhat consistent line exposure size as small as 10 μm s. Inconsistency arose with the washing or exposure process at some point resulting in the channels between exposed lines not always being clear of uncured resin as can be seen in the channels particularly on the right of this pattern.

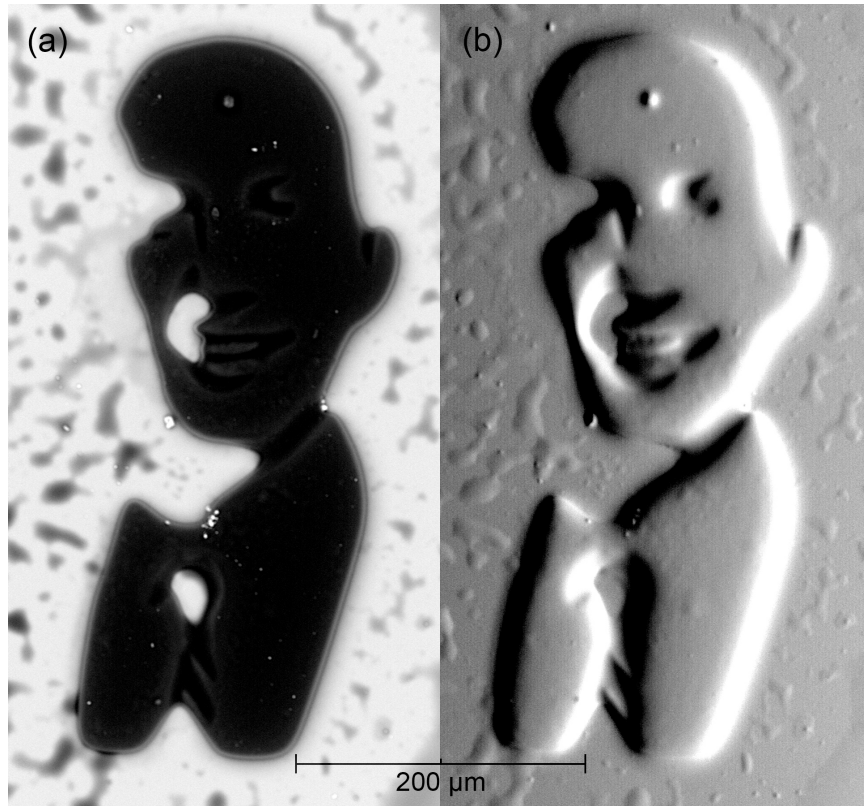


Figure 3.4: A 200µm wide profile of Dr. Tony Butterfield under (a) BSD and (b) topographical SEM imaging

To further demonstrate the variety of pattern and potential resolution, we etched [Figure 3.4](#). This etch showcases a profile of one of the advisors for this project, Dr. Anthony Butterfield. Note that the visible stripes on his tie lie just below that 10 µm range. The topographical view in [Figure 3.4b](#) provides a more clear picture of the actual resin shape on the surface with the illumination coming from the right of the image casting shadows to the left.

4 - DISCUSSION

The results of this project demonstrate that the developed lithostepper is capable of producing micro-scale features with a practical resolution approaching 10 μm . While this falls short of the theoretical diffraction-limited resolution of approximately 1 μm estimated via Rayleigh's criterion, the discrepancy can be attributed to a combination of material, optical, and process limitations inherent in the current system configuration.

A key factor influencing the practical resolution was the choice of UV-curable 3D printer resin, specifically Anycubic Standard Black Resin V2 as a substitute for traditional photoresist. While this resin offered a safer, fume-hood-free workflow and strong responsiveness to the 410 nm light source, its lower contrast, limited resolution, and development behavior introduced patterning artifacts that reduced feature fidelity and resolution. The lack of time to further develop optimized process control steps, such as precise exposure dose calibration or resist adhesion layers, further constrained pattern sharpness and reproducibility.

Nevertheless, the device successfully demonstrated critical photolithographic functions: dynamic pattern exposure via DMD projection, micron-scale alignment accuracy, and reproducible spin-coated layers. Multi-pattern tiling and recognizable etch structures illustrate the flexibility and creative control afforded by the system. ImageJ and SEM-based analysis confirmed repeatable feature sizes down to 10 μm , validating the core design and integration of optics, mechanical stages, and custom software.

Importantly, while this implementation achieved features down to 10 μm , similar systems built by other collaborators using the same HackerFab Lithostepper V2 architec-

ture—paired with traditional photoresist on silicon substrates—have demonstrated feature sizes in the 3–4 μm range. These results, more closely aligned with Rayleigh’s theoretical limit, and suggest that the hardware platform is fundamentally capable of finer resolution. The discrepancy highlights that the current limitations stem largely from the chosen materials and process environment rather than from the optics or stage mechanics themselves.

Overall, the results validate the system as a low-cost, flexible microfabrication tool that performs reliably within a 10 μm regime under simplified, resin-based conditions. They also provide a clear path for future improvement through material substitution, exposure refinement, and environment optimization, potentially unlocking sub-5 μm resolution capabilities already observed in parallel implementations.

One of the most compelling strengths of the lithostepper developed in this project is its exceptional cost-to-capability ratio. With a total build cost of approximately \$3,000, the system achieves resolution and patterning functionality comparable to tools that are orders of magnitude more expensive. A rough breakdown of this cost includes \$1,100 for the digital light processing (DLP) projector, \$800 for optical components such as the microscope objective and beamsplitter setup, \$700 for the high-resolution camera, \$300 for the XYZ stage and motorization hardware, and around \$100 for miscellaneous items including UV LEDs, PCBs, 3D-printed mounts, and wiring. A complete and actively maintained bill of materials is available on the [HackerFab Gitbook](#), as the design continues to evolve with ongoing contributions from the community.

Another significant advantage is the maskless, programmable exposure system. The integration of a Digital Micromirror Device (DMD) through the projector modification allows for dynamic pattern projection via HDMI, eliminating the need for expensive and

time-consuming photomask fabrication. This feature is particularly powerful for research and educational settings, where iterative design and rapid prototyping are essential. Patterns can be changed on-the-fly, enabling users to move from design to exposure in a matter of minutes, with no physical mask turnaround time.

The open-source foundation and modular architecture of the system further enhance its utility and accessibility. By basing the build on the Lithostepper V2 project from HackerFab, the device inherits a community-driven design philosophy, complete with publicly available design files, bill of materials, and firmware/software repositories. This ensures that the platform can evolve alongside contributions from other researchers and institutions, and that users can modify or troubleshoot the system without vendor lock-in or proprietary constraints. Additionally, it gave our project a community to contribute back to beyond our own university as work was completed on our device, results and struggles were reflected in updates to the build instructions in collaboration with HackerFab.

In terms of operation, the custom software interface provides an intuitive and unified control platform. Developed using Python and Tkinter, the software integrates camera feedback, XYZ stage movement, pattern uploading, and multi-layer alignment tracking in a single interface. Features such as Sobel-based focus scoring and exposure tiling greatly enhance usability and precision and are remarkable features for a system at this price point.

Finally, the simplicity of the supporting systems, including the spincoater and XYZ stage, is a strength in its own right. By using a modified hard drive motor, Arduino-based controls, and 3D-printed mounts, the spincoater provides reliable and repeatable thin film deposition for less than \$35. Similarly, the stage's capacitive homing sensors and GRBL firmware allow for precise, programmable, and absolute motion without complex calibra-

tion procedures.

Taken together, these strengths establish the lithography stepper as a powerful, low-barrier tool for photolithographic research and instruction. Its flexibility, affordability, and open-source design make it uniquely positioned to fill the gap between high-end nanofabrication infrastructure and the growing demand for decentralized microfabrication capabilities. While the stepper demonstrates promising capabilities, several intrinsic and implementation-based limitations currently constrain its performance and reliability.

The most immediate limitation stems from the choice of UV-curable resin in place of standard photoresists. Although selected for its ease of handling and compatibility with non-cleanroom environments, the resin lacks the resolution, contrast, and process stability of chemically engineered resists. It is more prone to partial development, edge blurring, and inconsistent feature formation, especially at smaller scales. This was particularly clear in SEM imaging, where some narrow channels between exposed features remained partially filled with residual resin, likely due to swelling, underdevelopment, or a failure to properly wash the substrate. Furthermore, the resin's high viscosity and general chemistry limit its sensitivity to precise dosage control, which is critical for producing features near the theoretical resolution limit.

Mechanically, while the XYZ stage performed adequately for controlled motion and repeatable tiling, its DIY motorization introduces alignment challenges and stage drift. Backlash, stepper motor vibrations, and thermal expansion effects can affect repeatability and long-term stability, especially during multi-layer alignment. Although the GRBL-based system supports homing and absolute positioning, the lack of closed-loop feedback or active compensation mechanisms makes fine-alignment between layers less robust compared

to commercial systems.

In the optical system, several practical limitations emerge. The use of off-the-shelf lenses and mounts, though cost-effective, introduces potential for aberrations and misalignment, our device even requiring a shim to ensure alignment. Achieving and maintaining sharp focus across the entire field of view requires meticulous manual adjustment, and the current setup could benefit from improved z-axis focusing and real-time correction. Moreover, the system's current numerical aperture (NA) is limited by the choice of a 10x microscope objective, constraining its theoretical resolution despite the 410 nm light source.

On the software side, limitations arise from the use of proprietary components. The camera integration relies on Teledyne's Spinnaker SDK, which is not open-source and complicates deployment across different platforms or institutions as code written to interface with it cannot be freely distributed. This is currently being worked on and fixed by HackerFab in switching to a camera with an open-source API. Additionally, while the current software provides core functionality such as pattern loading, focus scoring, and exposure control, it lacks advanced features like automated overlay registration, adaptive exposure calibration, or real-time image analysis—features that would significantly improve usability for multilayer or high-precision work.

Finally, environmental conditions and lab infrastructure play a non-negligible role. Operating the device in a non-cleanroom setting increases the risk of particulate contamination, inconsistent film deposition, and optical misalignment. These factors, while manageable, introduce noise and variability that must be accounted for in both experimental design and interpretation of results.

Collectively, these limitations highlight areas for improvement in both hardware and

process development. However, many of these challenges are not fundamental to the system architecture and can be addressed incrementally through improved materials, mechanical upgrades, and software enhancements, several of which are already underway in parallel HackerFab implementations. While the device has demonstrated substantial promise as a low-cost, maskless photolithography tool, several clear paths exist for future improvements that could dramatically enhance its usability, precision, and overall performance.

One of the most impactful upgrades would be reorienting the system to a vertical configuration. Currently, the device operates with the optical path horizontal across the lab bench, requiring the sample stage and optics to be manually aligned and secured in that plane. This layout not only consumes more space but also introduces mechanical sag, vibration sensitivity, difficulty in substrate holding, and alignment drift over time. Transitioning to a vertically mounted architecture would allow gravity to act perpendicular to the stage plane, significantly improving stage accuracy, focus stability, and ease of use particularly in alignment and multi-layer operation.

Another substantial improvement would be the integration of standard photoresists. While UV-curable resin was used for accessibility in this implementation, moving to industry-standard positive or negative resists would unlock the full optical resolution of the system. These materials, when used in conjunction with post-exposure bake and development processes such as using an adhesion promoter like HDMS, offer higher contrast, better-defined edges, and more predictable behavior during pattern transfer. This transition would also enable direct comparison with other HackerFab implementations already achieving sub-5 μm resolution using photoresist on silicon wafers.

On the mechanical side, upgrading the XYZ stage to include closed-loop feedback or

higher precision actuators would greatly enhance repeatability and layer alignment accuracy. Although the current stage with capacitive homing provides a strong foundation, incorporating encoders or high-resolution lead screws could reduce positional error and drift during longer or multi-step exposures.

For the optical system, experimentation with higher numerical aperture microscope objectives would allow for improved resolution, bringing the system closer to the theoretical $1\ \mu\text{m}$ diffraction limit. This would require corresponding changes in optical alignment and working distance, as well as refinement of the focusing feedback system to accommodate shallower depths of field, an implementation which would make the device much more modular than it currently is.

In terms of software development, future versions could expand functionality to include automated overlay correction, advanced focus routines, and real-time alignment guides. Improved automation, such as auto-calibration routines for exposure timing, stage mapping, and z-height determination, would streamline user workflow and reduce setup time, particularly for less experienced users or classroom settings.

Finally, enhancements to the spincoating process like incorporating a vacuum chuck for more consistent substrate mounting or enabling programmable multi-step spin profiles would improve film uniformity and make the system more robust for thinner resist applications. Our current spin coating setup is lacking in control over the process as a result of the limited time spent developing its firmware. These modifications could be made without need to modify the hardware we have created.

Collectively, these improvements represent practical and attainable next steps for evolving the system from a functioning prototype to a polished and versatile research tool. As

with much of the HackerFab initiative, the modular and open nature of the design supports further development and collaboration, allowing users to tailor the system to their specific use cases while contributing to a growing ecosystem of shared hardware and software innovation.

The development of this low-cost, maskless photolithography stepper has broader implications that extend well beyond the immediate technical scope of the project. Most notably, it underscores the potential and trend towards democratizing access to microfabrication tools, enabling hands-on experimentation and innovation in environments traditionally excluded from semiconductor research.

High-end photolithography tools are often centralized in national laboratories, elite research institutions, or multi-billion-dollar foundries. This consolidation creates a significant accessibility gap, especially for small startups, independent researchers, and educational institutions without cleanroom infrastructure. By contrast, the system developed here offers an alternative: a platform that, while modest in cost, provides a hands-on gateway into the world of optics, lithography, patterning, and MEMS fabrication.

In educational settings, the device offers an opportunity to bridge the divide between theory and practice. Concepts such as diffraction limits, resist chemistry, image alignment, and optical focusing that are often taught abstractly, become tangible and experiment-driven. With its live camera feedback, modular stage control, and visible results under basic microscopy, the stepper facilitates a level of engagement and understanding that is difficult to achieve through textbooks or simulations alone.

Beyond the classroom, the system holds value for early-stage hardware prototyping and interdisciplinary research, especially in fields like microfluidics, MEMS, photonics, and

lab-on-a-chip development. The ability to quickly pattern, modify, and re-pattern designs without photomasks significantly reduces iteration time, encouraging exploration of novel structures and process workflows with in-house accessible tools. This kind of agility is essential for applications at the intersection of materials science, chemistry, biology, and electrical engineering—fields increasingly reliant on rapid, micro-scale fabrication.

Furthermore, this project reflects a broader shift toward open hardware and distributed fabrication, echoing trends already present in software, electronics, and 3D printing. By building upon open-source platforms like HackerFab and contributing to a shared knowledge base, this work helps foster a collaborative and transparent ecosystem in which tools are not only used but actively improved and reshaped by their users. In this way, the system contributes to a growing movement aimed at making advanced manufacturing not just smaller and cheaper, but more inclusive and participatory. In a world where hardware innovation is increasingly gated by cost and infrastructure, accessible tools like this stepper may prove crucial in flattening the innovation curve, allowing more diverse ideas and contributors to participate in shaping the future of microscale technology.

BIBLIOGRAPHY

- [1] Helmut Gernsheim, *The History Of Photography*. 1955.
- [2] C. G. Willson, R. R. Dammel, and A. Reiser, “Photoresist materials: A historical perspective,” in *Advances in Resist Technology and Processing XIV*, vol. 3049, SPIE, Jul. 1997, pp. 28–41. DOI: [10.1117/12.275826](https://doi.org/10.1117/12.275826).
- [3] J. W. Lathrop, “The Diamond Ordnance Fuze Laboratory’s Photolithographic Approach to Microcircuits,” *IEEE Annals of the History of Computing*, vol. 35, no. 1, pp. 48–55, Jan. 2013, ISSN: 1934-1547. DOI: [10.1109/MAHC.2011.83](https://doi.org/10.1109/MAHC.2011.83).
- [4] A. Jules, “Fabrication of semiconductor devices,” US3122817A, Mar. 1964.
- [5] J. Griffin, E. Spooner, and H. Hassan, *Spin Coating: Complete Guide to Theory and Techniques*, <https://www.ossila.com/pages/spin-coating>.
- [6] R. and, “XXXI. Investigations in optics, with special reference to the spectroscope,” *The London, Edinburgh, and Dublin Philosophical Magazine and Journal of Science*, vol. 8, no. 49, pp. 261–274, Oct. 1879, ISSN: 1941-5982. DOI: [10.1080/14786447908639684](https://doi.org/10.1080/14786447908639684).
- [7] G. M. Blumenstock, C. Meinert, N. R. Farrar, and A. Yen, “Evolution of light source technology to support immersion and EUV lithography,” in *Advanced Microlithography Technologies*, vol. 5645, SPIE, Jan. 2005, pp. 188–195. DOI: [10.1117/12.577587](https://doi.org/10.1117/12.577587).

- [8] *C.L. Henderson Group - Introduction to Chemically Amplified Photoresists*, <https://sites.google.com/site/hendersonresearchgroup/helpful-primers-introductions/introduction-to-chemically-amplified-photoresists>.
- [9] P. D. Bisschop and E. Hendrickx, “Stochastic effects in EUV lithography,” in *Extreme Ultraviolet (EUV) Lithography IX*, vol. 10583, SPIE, Mar. 2018, pp. 350–366. DOI: [10.1117/12.2300541](https://doi.org/10.1117/12.2300541).
- [10] M. P. Stoykovich, H. Kang, K. C. Daoulas, *et al.*, “Directed Self-Assembly of Block Copolymers for Nanolithography: Fabrication of Isolated Features and Essential Integrated Circuit Geometries,” *ACS Nano*, vol. 1, no. 3, pp. 168–175, Oct. 2007, ISSN: 1936-0851. DOI: [10.1021/nn700164p](https://doi.org/10.1021/nn700164p).
- [11] PatentPC, *Chip Manufacturing Costs in 2025-2030: How Much Does It Cost to Make a 3nm Chip?* <https://patentpc.com/blog/chip-manufacturing-costs-in-2025-2030-how-much-does-it-cost-to-make-a-3nm-chip>, Apr. 2025.
- [12] A. Tsiamis, Y. Li, C. Dunare, *et al.*, “Comparison of Conventional and Maskless Lithographic Techniques for More than Moore Post-Processing of Foundry CMOS Chips,” *Journal of Microelectromechanical Systems*, vol. 29, no. 5, pp. 1245–1252, Oct. 2020, ISSN: 1941-0158. DOI: [10.1109/JMEMS.2020.3015964](https://doi.org/10.1109/JMEMS.2020.3015964).
- [13] C. Weber, C. Berglund, and P. Gabella, “Mask Cost and Profitability in Photomask Manufacturing: An Empirical Analysis,” *Semiconductor Manufacturing, IEEE Transactions on*, vol. 19, pp. 465–474, Dec. 2006. DOI: [10.1109/TSM.2006.883577](https://doi.org/10.1109/TSM.2006.883577).

- [14] M. Kang, C. Han, and H. Jeon, *Submicrometer-scale pattern generation via maskless digital photolithography*,
<https://opg.optica.org/optica/fulltext.cfm?uri=optica-7-12-1788&id=444830>.
- [15] *The Hacker Fab at Carnegie Mellon University – The first open-source semiconductor fab*, <https://hackerfab.ece.cmu.edu/>.
- [16] *DLPDLCR471TPEVM Evaluation board — TI.com*,
<https://www.ti.com/tool/DLPDLCR471TPEVM>.
- [17] Y.-T. Tu, *Simulator - Ray Optics Simulation*,
<https://phydemo.app/ray-optics/simulator/>.
- [18] M. Brinkmann, J. Hayden, M. Letz, *et al.*, “Optical Materials and Their Properties,” in *Springer Handbook of Lasers and Optics*, F. Träger, Ed., New York, NY: Springer, 2007, pp. 249–372, ISBN: 978-0-387-30420-5. DOI: [10.1007/978-0-387-30420-5_5](https://doi.org/10.1007/978-0-387-30420-5_5).
- [19] *Digital Micromirror Device - an overview — ScienceDirect Topics*,
<https://www.sciencedirect.com/topics/engineering/digital-micromirror-device>.
- [20] *Spinnaker SDK — Teledyne Vision Solutions*,
<https://www.teledynevisionsolutions.com/products/spinnaker-sdk/?model=Spinnaker%20SDK&vertical=machine%20vision&segment=iis>.
- [21] *Gnea/grbl*, gnea, Apr. 2025.
- [22] *Hacker-fab/stepper*, Hacker Fab, Apr. 2025.

- [23] C. Mo and B. Liu, “An auto-focus algorithm based on maximum gradient and threshold,” in *2012 5th International Congress on Image and Signal Processing*, Oct. 2012, pp. 1191–1194. DOI: [10.1109/CISP.2012.6469961](https://doi.org/10.1109/CISP.2012.6469961).
- [24] C. T. Rueden, J. Schindelin, M. C. Hiner, *et al.*, “ImageJ2: ImageJ for the next generation of scientific image data,” *BMC Bioinformatics*, vol. 18, no. 1, p. 529, Nov. 2017, ISSN: 1471-2105. DOI: [10.1186/s12859-017-1934-z](https://doi.org/10.1186/s12859-017-1934-z).

Name of Candidate: John Peterson

Date of Submission: April 23, 2025